Population of hyperdeformed structures in ^{152}Dy from proton-gamma coincidence experiments

G. Viesti, M. Lunardon, D. Bazzacco, R. Burch, D. Fabris, S. Lunardi, N. H. Medina, G. Nebbia, and C. Rossi-Alvarez
INFN and Dipartimento di Fisica dell'Universitá di Padova, I-35131 Padova, Italy

G. de Angelis, M. De Poli, E. Fioretto, G. Prete, J. Rico, P. Spolaore, and G. Vedovato
INFN Laboratori Nazionali di Legnaro, I-35020 Legnaro, Padova, Italy

A. Brondi, G. La Rana, R. Moro, and E. Vardaci
INFN and Dipartimento di Fisica dell'Universitá di Napoli, I-80125 Napoli, Italy
(Received 22 November 1994)

The ridge structure with $\Delta E_\gamma = \pm 30$ keV, recently observed in the reaction 187 MeV ^{37}Cl+^{120}Sn and attributed to a hyperdeformed nuclear shape, has been confirmed in a new proton-γ coincidence experiment and assigned to the ^{152}Dy nucleus. Estimates of the cross section for the population of the 30 keV ridge and for the associated entry states have been obtained. The proton spectra in coincidence with γ rays of different Dy isotopes show effects related to the exit channel and to the angular momentum but they are scarcely sensitive to the selection of different shapes (oblate, normal deformed prolate, superdeformed) in the same residual nucleus ^{152}Dy. The energy of the protons in coincidence with the $\Delta E_\gamma = \pm 30$ keV ridge is however larger than expected. This effect is discussed in the framework of the fission-evaporation competition.

PACS number(s): 27.70.+q, 21.10.Re, 25.70.Gh

I. INTRODUCTION

Rotational bands built upon hyperdeformed (HD) shapes (axis ratios 3:1) are predicted in nuclei by theories which successfully explain the occurrence of superdeformed (SD) nuclear states and their properties [1,2]. According to the calculations, the HD bands should be yrast at angular momenta larger than $70\hbar$: consequently it is expected that their experimental identification is extremely difficult fission being the dominant channel at this angular-momentum regime. The search for such exotic shapes is therefore not only interesting in itself but might be useful in defining the behavior of the fission probability (and hence of the fission barrier) at very high spin as it should yield information on the survival probability of the HD states.

As in the case of superdeformation [3], the first experimental signature for hyperdeformation was the observation of a ridge structure in an E_γ-E_γ correlation matrix [4]. The hyperdeformed ridge, which was identified in an experiment performed at Chalk River using the reaction ^{37}Cl $+^{120}$ Sn at 187 MeV, is located at $\Delta E_\gamma = E_\gamma 1 - E_{\gamma 2} = \pm 30 \pm 3$ keV corresponding to a dynamical moment of inertia $J^2 \sim 130\hbar^2$ MeV^{-1}. The ridge at ± 30 keV could be observed only requiring the coincidence with a proton as suggested in [1]. The Chalk River group proposed also a cascade of 10 discrete lines with an average energy spacing of 30 keV. This first experiment could however not be conclusive for the assignment of the HD structure to a specific nucleus although the choice was limited to the ^{152}Dy and ^{153}Dy nuclei.

We report here on the results of a new proton-gamma coincidence experiment which was performed, using the same reaction of Ref. [4], with the goal to confirm that earlier observation and to assign the $\Delta E_\gamma = \pm 30$ keV ridge to one of the two proposed nuclei. In our experiment we studied in detail the proton spectra in coincidence with different evaporation residues and/or different bands in the same nucleus, in order to search for structure effects in the proton emission. Finally, the energy of protons in coincidence with the $\Delta E_\gamma = \pm 30$ keV has been compared with that of protons in coincidence with other shapes in the residual nuclei to shed light on the population mechanism of such exotic shapes.

II. EXPERIMENTAL DETAILS

The experiment has been performed at the XTU Tandem facility in Legnaro. Gamma rays were detected with the GASP spectrometer [5], which consists of an array of 40 large-volume Compton-suppressed Ge detectors and of an inner ball of 80 Bismuth Germanate (BGO) crystals. A beam of 187 MeV ^{37}Cl (intensity 1–3 pnA) was focused onto a stacked target composed by two 500 μg/cm^2 foils of ^{120}Sn.

Charged particles have been detected in a light-particle hodoscope (LPH) consisting of 8 silicon detectors, 300 μm thick, each one with a size 6 cm×4 cm. The detectors were closely packed to form a 18 cm×18 cm wall which was placed at 8 cm downstream of the target. Particles emitted at $\theta_{\rm lab} \sim 10°$–$50°$ were detected with a geometrical efficiency of $\sim$ 90%. In this reaction the forward emitted protons are not stopped in the LPH; therefore,

 ©1995 The American Physical Society

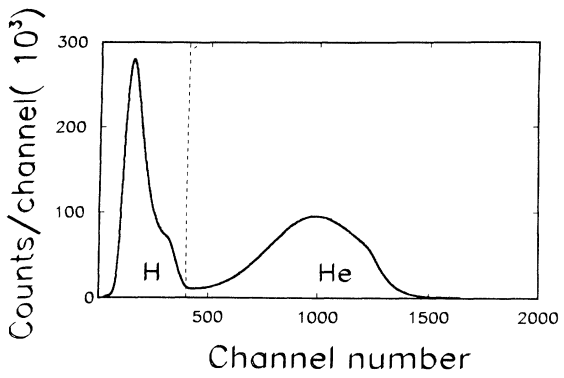

FIG. 1. Sample raw spectrum of the LPH obtained summing events from the eight silicon detectors. The vertical dashed line corresponds to the threshold used in the data analysis to discriminate between protons and alpha particles.

a good discrimination between protons and alpha particles could be achieved simply from the energy loss in the Si detectors, as shown in Fig. 1. Heavier particles and scattered beam ions were stopped in a 13-mg/cm^2-thick Mylar absorber placed in front of the Si detectors.

An additional large area telescope (LAT) made by three 5 cm×5 cm silicon detectors (300, 1000, 1000 μm thickness) was also placed at $\theta_{\rm lab} \sim 70°$.

Approximately 800×10^6 events, consisting of triples or higher-fold Ge coincidences with multiplicity $k > 3$ on the BGO ball, were collected in an 8-day run. Because of the limited solid angle covered by the particle detectors and of the low cross section of the *xpyn* channels ($\sim 20\%$ of the total evaporation residue yield), only 25×10^6 and 0.45×10^6 of the collected events were in coincidence with protons detected in the LPH and in the LAT, respectively.

III. THE 30 keV RIDGE

Using different gating conditions on the γ-ray sum energy (H) and fold (k) registered in the BGO ball, various E_γ-E_γ matrices were produced from the proton-gated triples Ge data. Cuts perpendicular to the main diagonal $E_{\gamma 1} - E_{\gamma 2}$ were subsequently made on these matrices in order to observe the ridges corresponding to deexcitations of the final nuclei along particular rotational structures. This analysis has been performed both on the original proton gated matrices and on those obtained after background subtraction which follows, as in [4], the procedure of Palameta and Waddington [6]. The data have not been corrected for the Ge γ-ray efficiency.

With a cut in the energy range $1200 \leq (E_{\gamma 1}+E_{\gamma 2})/2 \leq 1325$ keV we clearly see the well-known ridge located at 48 keV from the diagonal [see Fig. 2(a)]. This ridge results from transitions between the levels of the well-known, discrete ^{152}Dy [7] and ^{153}Dy [8] SD bands. The transitions of the ^{152}Dy SD band which are inside the

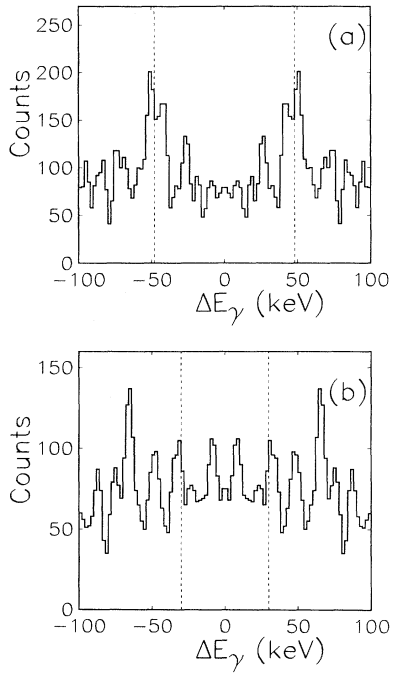

FIG. 2. Spectra of $\Delta E_\gamma = E_{\gamma 1} - E_{\gamma 2}$ corresponding to diagonal cuts in the E_γ-E_γ coincidence matrix generated with conditions on sum energy $H > 14$ MeV and fold $k > 10$ on the inner ball. The matrix has been background subtracted following [6]. The spectrum (a) corresponds to a cut in the energy range $1200 \leq (E_{\gamma 1} + E_{\gamma 2}/2 \leq 1325$ keV; the spectrum (b) corresponds to a cut in the energy range $1375 \leq (E_{\gamma 1} + E_{\gamma 2})/2 \leq 1500$ keV.

cut limits account for $\sim 40\%$ of the total 48 keV ridge intensity. The feeding pattern of the yrast SD band populated by the $1p4n$ channel has been compared with that measured in the $4n$ channel of the reaction 205 MeV ^{48}Ca $+^{110}$ Pd as reported by Bentley *et al.* [9]. The two feeding patterns appear to be identical within the experimental uncertainties.

We made also a cut in the energy range $1375 \leq (E_{\gamma 1} + E_{\gamma 2})/2 \leq 1500$ keV, the same as in [4]. The conditions used in the data sorting, $H > 14$ MeV and $k > 10$, should correspond to those of [4] if one takes into account the different efficiency of the inner balls of the two experiments. In the resulting spectrum shown in Fig. 2(b), many ridges are observed, among them one at $\Delta E_\gamma = \pm 32 \pm 3$ keV.

A two-dimensional correlation technique has been used in order to check in this ridge is due to a rotational cascade based on an hyperdeformed nuclear shape or if, instead, it can originate from coincidences between few discrete transitions.

Figure 3 shows the results of this analysis. After summing six diagonal cuts, each 5 keV wide, separated by 30 keV in the $E_\gamma \geq 1250$ keV region we observe an enhancement of the 30 keV ridge when the cuts are at some definite energies. Figure 3(a) reports the area of the 30

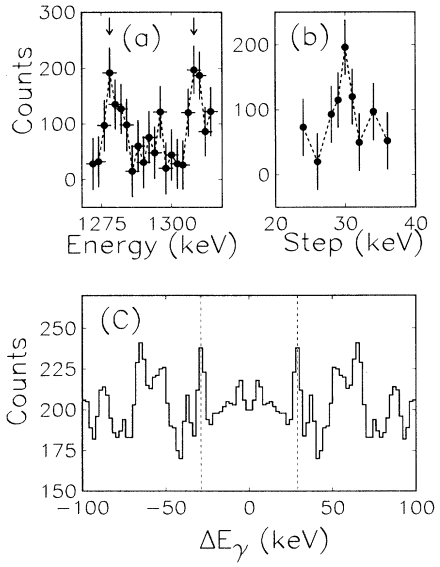

FIG. 3. Area of the 30 keV ridge in the spectra obtained summing the grid of six diagonal cuts 5 keV wide as a function (a) of the energy of the first cut and (b) the grid step. The E_γ-E_γ coincidence matrix generated with conditions $H > 14$ MeV and $k > 10$ but without background subtraction is used. The ΔE_γ spectrum obtained when summing the six cuts with the 30 keV step and with the first cut at the energy of the maximum in (a) is shown in (c).

keV ridge as a function of the energy of the first of the six cuts. The maxima at cut energies $\sim 1278 + (n \times 30)$ keV ($n = 0, 1, \ldots, 5$) suggest the presence of a rotational cascade with $\Delta E_\gamma = 30$ keV and with transition energies $\sim 1263 + (n \times 30)$ keV. Such energies are compatible with those listed in [4] for the proposed members of the HD band. Of course, the energy difference between consecutive cuts has been also varied [see Fig. 3(b)], but the 30 keV ridge is clearly observed, as shown in Fig. 3(c), only when the above-mentioned conditions ($\Delta E_\gamma = 30$ keV and first cut at 1278 keV) are satisfied.

In this way we have found that the part of the 32 keV ridge at $\Delta E_\gamma = 30$ keV is due to events correlated in a rotational sequence. We found also that, because of some strong coincident transitions with $\Delta E_\gamma = 32$ keV which lie in the energy range $1375 \leq (E_{\gamma 1} + E_{\gamma 2})/2 \leq 1500$ keV, a sizable part of the 32 keV ridge intensity is due to the contribution of only a pair of cuts.

Using the procedure outlined above we have spanned the $24 \leq \Delta E_\gamma \leq 55$ keV region obtaining similar results also for the superdeformed ridge at 48 keV (i.e., maximum intensity when the energy difference between cuts is 48 keV and the position of the first cut corresponds to one of the transition energies of the yrast SD band of ^{152}Dy). In this way we can compare the intensity of the HD ridge to that of the SD one. Taking into account that in the energy region of interest the ^{152}Dy superdeformed band contributing to the 48 keV ridge is at $\sim 50\%$ of its maximum intensity, we can extract a relative intensity ratio HD:SD of $\sim 10\%$.

No definite assignment of the HD ridge to either ^{152}Dy or ^{153}Dy has been possible from the data of [4]. We have therefore reanalyzed our data in order to assign the 30 keV ridge to one of the two nuclei. From the $(2k)^3$ symmetrized cube, obtained from the events in coincidence with protons and setting a condition $k > 5$ in the inner ball, we have produced several E_γ-E_γ matrices gating on the prominent discrete lines of the different Dy isotopes. The ridge spectra have been obtained from those matrices with or without performing the background subtraction of [6], producing equivalent results. In particular the spectra shown in Fig. 4 are those obtained without background subtraction.

The hyperdeformed ridge is clearly visible in the matrix with no conditions on the third gamma [see Fig. 4(a)] which accounts for 52×10^6 events. When gating on the prominent lines of ^{152}Dy above the $\tau = 60$ ns 17^+ isomer (148, 211, 254, 403, 541, 685, and 991 keV), a matrix with only 3.4×10^6 events is obtained. Despite the reduced statistics, the ridge stands clearly as shown in Fig. 4(b). On the other side, only few counts are present at $\Delta E_\gamma = \pm 30$ keV in the matrices obtained with gates set on prominent lines of the other Dy isotopes [see Figs. 4(c) and 4(d)]. We stress that the yield of the ridge in Figs. 4(a) and 4(b) is distributed rather uniformly over all the six cuts. The results reported in Figs. 4(a)–4(d) clearly demonstrate that the proposed HD band which originates the ridge at $\Delta E_\gamma = \pm 30$ keV belongs to the

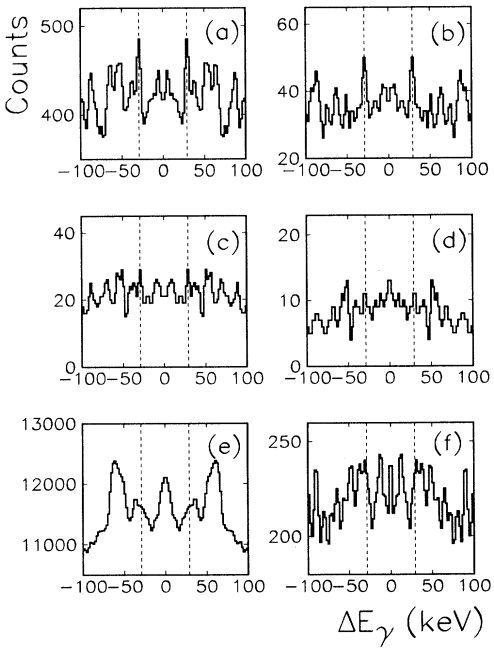

FIG. 4. The 30 keV ridge in the spectra obtained in coincidence with protons: (a) without gates on discrete lines; (b) with gates on the prominent transitions in ^{152}Dy; (c) with gates on the prominent transitions in^{150,151,153}Dy; and (d) with gates on the prominent transitions in ^{153}Dy nucleus. E_γ-E_γ coincidence matrices are generated with the condition $k > 5$ (without background subtraction). The spectra (e) and (f) are obtained using the same conditions as (a) and (b) but without proton tagging.

^{152}Dy nucleus.

In order to show the importance of the proton tagging we present also ridge spectra from an analysis of the collected data which did not require the coincidence with protons detected in the LPH. The obtained spectra which are shown in Figs. 4(e) and 4(f) are equivalent to those of Figs. 4(a) and 4(b), respectively. The inclusive spectrum of Fig. 4(e) shows only very broad structures; the spectrum of Fig. 4(f), obtained setting gates on prominent transitions in the ^{152}Dy nucleus, is rather cleaner but the presence of the $\Delta E_\gamma = \pm 30$ keV ridge can hardly be recognized. This shows that the selectivity obtained using gating conditions on discrete gamma transitions is not sufficient to reject interfering structures which, as a matter of fact, are eliminated only by the coincidence with protons.

Statistical model calculations predict for the reaction 187 MeV ^{37}Cl $+^{120}$ Sn a cross section of 50 mb for the production of the ^{152}D isotope, out of a total fusion evaporation cross sections of 750 mb. Taking into account that the population of the SD yrast band in ^{152}Dy accounts for $\sim 1\%$ of the total population of the nucleus, from the experimentally determined HD:SD ratio we obtain an estimated cross section for the population of the HD ridge of ~ 50 μb. This quantity corresponds to less than 1×10^{-4} of the fusion evaporation cross section, a figure which is at the limits of the present generation of γ-ray spectrometers.

The ^{152}Dy nucleus seems to be the best example of coexistence of the most varied nuclear shapes going from oblate noncollective with $\beta_2 \sim 0$ to hyperdeformed with $\beta_2 \sim 0.9$ through the intermediate deformation of $\beta_2 = 0.3$ (collective prolate shape) and $\beta_2 = 0.6$ (superdeformed shape).

The BGO inner ball has been used to study the entry state population associated with the different evaporation residues and with the different structures in the ^{152}Dy nucleus. In Fig. 5, average values of the fold k and sum energy H, as measured in coincidence with the relevant transitions in ^{150,1,2,3}Dy nuclei, are reported. As expected, the entry state population moves toward higher k and H values for the heavier isotopes due to the balance between the number of evaporated particles and the available excitation energy above the yrast line. The effect of the $\tau = 60$ ns isomeric state in reducing the k and H values, obtained in a thin target experiment, for the ^{152}Dy nucleus with respect to the neighboring isotopes is clear from the data points reported in Fig. 5. The entry state populations related to the oblate and to the SD states in the ^{152}Dy nucleus are reported in Fig. 6. It appears that the SD states are correlated, on average, to larger values of k and H with respect to the oblate states. We have verified, by using published branching ratios [9], that the difference between SD and oblate states cannot be completely explained by the branch of the SD population which bypasses the 60 ns isomer and corresponds to slightly different values of k and H.

Finally, we have studied the entry states correlated with the events in the 30 keV ridge. The ridge area (obtained by summing the six cuts) has been analyzed as a function of the lower threshold in the fold k and sum energy H used to extract the γ-γ matrices. The same analysis has been done also for the 48 keV ridge and for the strong discrete transitions in ^{152}Dy. The data are presented in Figs. 7(a) and 7(b) and show qualitatively that the 30 keV ridge, as expected, is associated with an entry region located at higher values of fold and sum energy with respect to the SD ridge. In this figure the average value of the k (or H) distribution associated with the different structures corresponds to $\sim 50\%$ of the relative yield. Statistical uncertainties on the ridge area as well as the saturation of the BGO inner ball response at high fold do not allow a more quantitative definition of the spin region associated with the 30 keV ridge. Nevertheless, a simple comparison with the SD data indicates that the average angular momentum for the 30 keV ridge should be certainly higher than $60\hbar$.

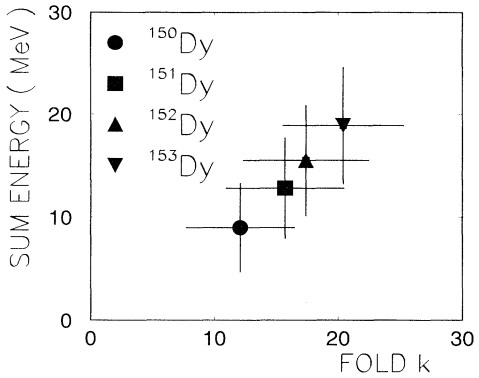

FIG. 5. Average entry state for the relevant Dy isotopes in the k vs H plane. The error bars are equal to the width (FWHM) of the distributions in k and H measured with the inner ball.

IV. PROTON SPECTRA FROM THE LARGE AREA HODOSCOPE

We have analyzed the ΔE proton spectra detected in the hodoscope by using fourfold coincidence events E_γ-E_γ-E_γ protons. As a first step we have studied the

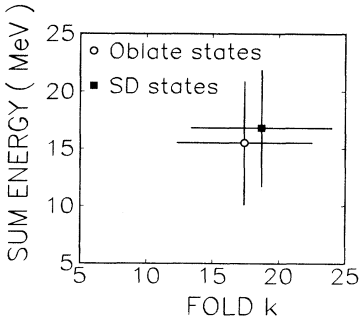

FIG. 6. As Fig. 4 but for oblate and SD states in the ^{152}Dy nucleus.

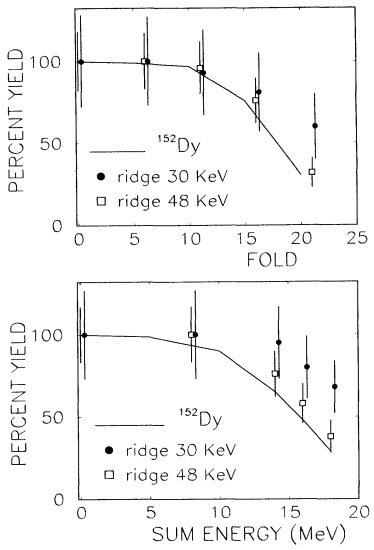

FIG. 7. Area of the 30 keV and 48 keV ridges as a function of the lower threshold in fold k and sum energy H used in generating the E_γ-E_γ coincidence matrices. Results for the corresponding relative population of oblate states in the ^{152}Dy nucleus are also reported.

spectra obtained by gating on the prominent transitions in the different Dy isotopes. In Fig. 8, the experimental spectra are reported and compared with the predictions of the Monte Carlo version [10] of the statistical model code CASCADE [11] in which the experimental geometry of the hodoscope is taken into account. The statistical model predicts that the average proton energy is decreasing with increasing number of emitted neutrons in the pxn channels. This effect can be simply understood by considering that the total available thermal excitation energy has to be shared between the number of evaporated nucleons because the proton is emitted, according to the model calculations, with equal probability along the deexcitation cascade. Therefore, the excitation energy carried away per evaporated particle increases for heavier residues giving a larger proton energy. The predicted trend is evident also in the experimental data [Fig. 8(b)], having in mind the energy loss nature of the spectra (i.e., the energy loss decreases with increasing energy of the protons).

In the following, we report the analysis of the proton spectra by using the first moment of the energy-loss distribution in the region of the evaporative peak, $\langle \Delta E \rangle$. This quantity is better correlated to the average energy of the evaporated protons than the value obtained when averaging over the complete energy-loss spectrum because of the nonlinear relation between energy and energy loss. The $\langle \Delta E \rangle$ values as a function of the evaporation residues are reported in Fig. 9(a).

A further selection can be obtained by gating on the discrete transitions of the final nuclei and for different windows in the fold k distribution. The general trend, revealed in Fig. 9(b), is that for a given number of emitted particles the average proton energy is shifted toward lower values when one selects higher fold (i.e., higher angular momentum) windows, a fact which is explained by the decrease of the available excitation energy above the yrast line. This trend is well reproduced by the calculations and is in agreement with the angular-momentum dependence of the proton spectra already evidenced in earlier investigations [12,13].

After observing the strong dependence of the proton

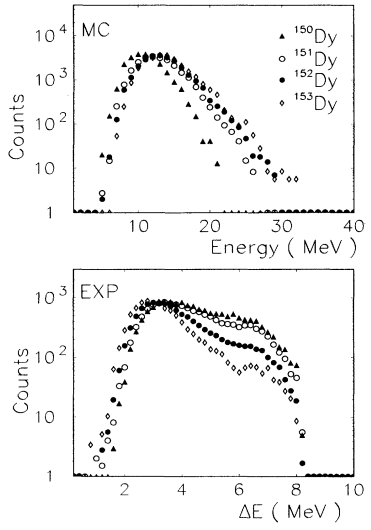

FIG. 8. Experimental energy-loss spectra of protons detected in the large area hodoscope in coincidence with the prominent transitions in the different Dy isotopes the hodoscope (lower panel). Proton energy spectra predicted from the Monte Carlo (MC) statistical model are reported in the upper panel for comparison.

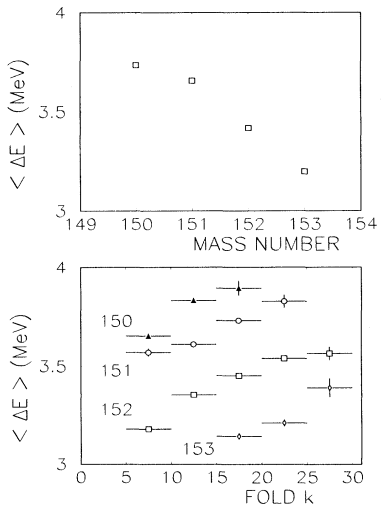

FIG. 9. Average values of the energy loss of protons detected in the large area hodoscope in coincidence with different pxn channels (upper panel) and windows in fold k (lower panel).

energy on the phase space available to the decay for the different pxn channels, we concentrated our attention on the proton spectra obtained by gating on the γ rays of the different structures (oblate, prolate, and SD) in the ^{152}Dy nucleus. The $\langle \Delta E \rangle$ values are shown in Fig. 10 as a function of the spin of the gating transition, J_{gate}. For the SD band the spin values suggested in Ref. [9] are used. The gate on the transition deexciting a state at spin J_{gate} selects all the entry states, and therefore the compound nucleus states from which the particle decay originates, with angular momentum $J \leq J_{\text{gate}}$. Consequently, the $\langle \Delta E \rangle$ values versus J_{gate} depend on the feeding pattern of each particular structure. With this in mind, some general features are clearly visible in Fig. 10.

(1) The measured $\langle \Delta E \rangle$ value increases (i.e., the average proton energy decreases) with angular momentum up to $J_{\text{gate}} \leq 40\hbar$ after which they flatten off. The $\langle \Delta E \rangle$ values determined in this way are within the limits obtained by setting gates on strong transitions deexciting low spin oblate states and windows on the lower (k = 5–10) and higher (k = 26–30) folds for which the ^{152}Dy nuclei are populated.

(2) The differences of the proton energy loss $\langle \Delta E \rangle$ in coincidence with the prolate, oblate, and SD bands are small for roughly equal entry spin region (i.e., the same J_{gate}).

These facts strongly support the picture of a complete decoupling between the earlier stage of the decay, when particles are emitted, and the near-yrast gamma cascade with the feeding of different classes of states [14]. This feature will be discussed in the next section where the proton spectra from the telescope are presented.

Among the different structures, the prolate one shows the largest sensitivity to the selection of J_{gate}. This means that the side feeding is important in the population of this band, and therefore that part of the population is derived from entry states at low angular momenta. On the contrary, the SD band shows a small variation of $\langle \Delta E \rangle$ with J_{gate}, suggesting that the bulk of the entry states are in this case at angular momenta larger than 50–60$\hbar$. This is in good agreement with the feeding pattern of the band measured in the present experiment as well as in previous experimental works [7,9].

We have also extracted the $\langle \Delta E \rangle$ values for the events which populate the 30 keV ridge. It has to be stressed that in this case the statistics is poor and that the background subtraction for the ridge events is critical. The result reported in Fig. 10 represents the value obtained averaging over several different ways of subtracting the background. We associate in Fig. 10 the $\langle \Delta E \rangle$ value obtained for the 30 keV ridge to angular momenta $J = 72 \pm 10\hbar$, which is the spin range suggested in [4] for the HD band. Although the experimental uncertainty is rather large, it seems that the protons in coincidence with the suggested hyperdeformed ridge are characterized by a lower $\langle \Delta E \rangle$, i.e., they are more energetic than expected from the simple extrapolation of other results for ^{152}Dy. In fact the spin range suggested in [4] for the ridge is larger than that associated to the SD band, as qualitatively also supported by the results of Fig. 7, and therefore a lower excitation energy is expected to be dissipated in the particle emission feeding the 30 keV ridge with respect to that related to the SD structure. We estimate an increase of about $\sim$ 0.5 MeV for the average proton energy in coincidence with the HD ridge with respect to the SD case.

V. PROTON SPECTRA FROM THE LARGE AREA TELESCOPE

Energy spectra of protons, detected in the LAT telescope, have been obtained in coincidence with the most prominent γ rays of the ^{150,151,152,153}Dy nuclei and with the oblate, prolate (normal deformed, ND) and SD bands in the ^{152}Dy nucleus. These data have lower statistics compared to those of the hodoscope; however they provide complementary information as the shape of the spectra is here more sensitive to the barrier and level density.

The proton spectra obtained gating on the γ transitions of ^{150,151,152,153}Dy isotopes are shown in Fig. 11. The spectra have been normalized for comparison to the same maximum. As already found with the hodoscope, we observe a decrease of the average energy with increasing number of emitted particles. The different slopes of the high-energy side of the spectra reflect the average temperature of the emitting nuclei, which decreases with increasing number of emitted particles. This behavior is

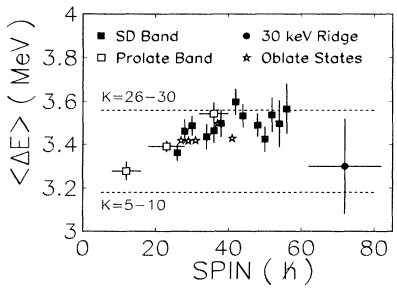

FIG. 10. Average energy loss for protons detected in the large area hodoscope in coincidence with different structures in ^{152}Dy as a function of the spin of the gating transitions. See text for details.

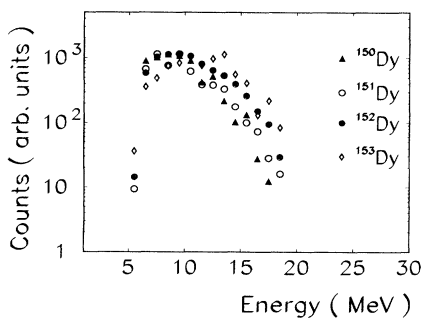

FIG. 11. Experimental energy spectra for protons detected in the large area telescope in coincidence with the relevant transitions of ^{150,151,152,153}Dy nuclei.

accounted for by the statistical model as shown in Fig. 12 where a comparison between the measured spectra and those calculated, taking into account the detection geometry of the telescope, is presented. The shape of the spectra is reasonably well reproduced by the model, although this latter shows the tendency to underestimate their low-energy side. The origin of this discrepancy, which was already observed in inclusive data [15], is still the object of controversial interpretations [16]. It is anyway important to notice the presence of such deviations also in selective data, like those of our experiment.

A comparison between the proton energy spectra obtained when gating on the different bands (oblate, prolate, and SD) in the ^{152}Dy nucleus is shown in Fig. 13. The shape of the energy spectra shows no significant variations with the nuclear shape, confirming the result obtained from the ΔE spectra. We do not observe any barrier reduction in the spectrum associated with the SD band when compared to that in coincidence with ND states. Similar results have been found for the ^{152}Dy and for the ^{133}Nd nuclei in [17]. In the $A \simeq 80$ mass region different experiments gave contrasting results in this respect. Large energy shifts and changes in the shape of proton spectra, obtained setting gates on different rotational bands, were reported in [12] for nucleus ^{82}Sr, while no evidence for structural effects on the proton spectra was found in [13] for the ^{81}Sr and ^{84}Zr nuclei.

In order to assess the sensitivity of proton spectra to nuclear deformation, we have performed calculations using the single step code GANES [18]. In this code the nuclear deformation is treated in a consistent way, using a Cassini shape parametrization. The spectra calculated assuming spherical or a deformed (axis ratio 2:1) compound nucleus ^{157}Ho are compared in Fig. 14. The model predicts an energy shift of about 1 MeV: this value is large enough to be experimentally observed, although it is expected to be reduced by the multistep emission. Indeed, four neutrons are emitted in our case. Besides the multistep emission, the peculiarities of the states populated by the proton emission could further reduce the

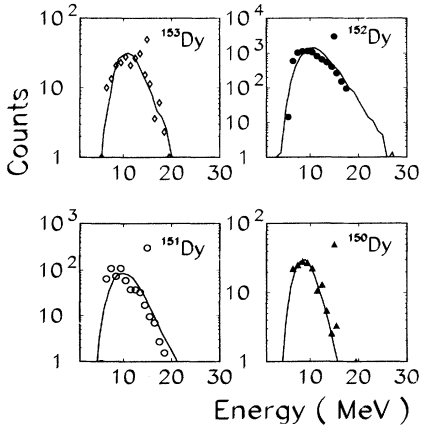

FIG. 12. Comparison between the proton energy spectra of Fig. 10 and the predictions from the statistical model CASCADE (Monte Carlo version).

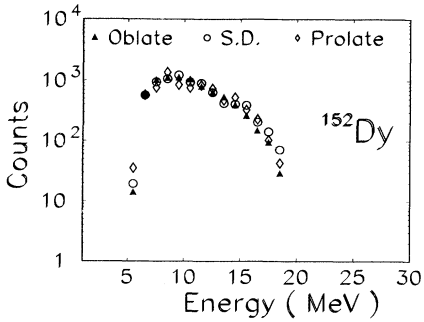

FIG. 13. Comparison between proton energy spectra from the large area telescope measured in coincidence with different bands in the ^{152}Dy nucleus.

expected shift in the barrier. In the framework of the statistical model [19], the difference in the proton spectra associated with the SD and the ND states should reflect the level densities of these states in the different excitation energy-angular-momentum regions populated by the protons. A ratio of level densities close to 1.0 for the SD and ND states has been adopted in [20] in order to reproduce the intensity ratios for the two bands, as a function of the excitation energy. Therefore, our result is consistent also with the findings of [20].

VI. DISCUSSION AND CONCLUSIONS

In recent calculations for ^{152}Dy the HD minimum appears at spin $60\hbar$ and becomes yrast at spin $\sim$ 80–$90\hbar$. It is therefore very interesting to study the conditions for which such extremely high spin values may be sustained by nuclei in elongated shapes without fissioning. Octupole correlations have been found [2] to be very large at hyperdeformed shapes for nuclei of the $A = 150$ region. A stable minimum is predicted for ^{152}Dy at $\beta_2 = 0.93$ and $\beta_4 = 0.13$. Calculations of the moments of inertia at this shape give a $J^{(2)}$ value of $130\hbar^2$ MeV^{-1}, very close to the rigid-body moment of inertia and in perfect agreement with the value extracted from the experimental data [4].

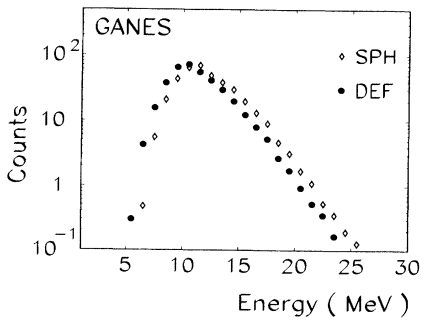

FIG. 14. Energy spectra of protons as simulated by the code GANES assuming spherical or deformed (axis ratio 2:1) compound nucleus ^{157}Ho.

In the present experiment the ^{157}Ho compound nucleus is populated at $E_x = 84$ MeV of excitation energy with a critical angular momentum $J_{\rm crit} = 77\hbar$. From systematics we derive that the boundary between evaporation and fission is around $J \sim 70\hbar$, being the fission channel centered around $\langle J^{\rm fission} \rangle = 74\hbar$. Therefore, the proposed range 62–82 $\hbar$ for the observed HD ridge [4] strongly overlaps with the fission region and extends up to the highest partial waves populated in the fusion reaction.

It is known, from experimental systematics, that in a reaction like the one studied here the prescission emission is dominated by dynamical effects and that the fission appears later in the deexcitation cascade [21,22]. Furthermore, the emission of protons prior to fission is strongly dependent from the excitation energy and seems to appear only in the path from the equilibrium to the saddle point and not in the saddle-to-scission transition [23]. It is therefore possible that the protons in coincidence with nuclei surviving fission at the highest angular momenta are emitted prevalently in the first step of the decay. On the contrary, the protons in "normal" statistical decay are, in model calculations, emitted with equal probability at any step of the cascade. This might be the origin of the experimentally observed increase in average energy for the events associated with the 30 keV ridge. Model calculations seems to support this hypothesis. In fact a difference of 700 keV of the average energy of protons feeding the ^{152}Dy nucleus from states at $J > 55\hbar$ is predicted between the first chance emission and the total decay chain.

The second point to be understood is the importance of the proton tagging in itself. The search for the HD ridge has been indeed unsuccessful in nuclei populated through xn channels [24]. We have verified that in those reactions the calculated spin distribution of the CN states which feed the ^{152}Dy final nucleus is very close to that of the ^{37}Cl+^{120} Sn reaction. Furthermore, the cross section for the population of the ^{152}Dy nucleus through the xn channels using ^{48}Ca beams on Pd targets is ~ 4 times larger than that of the $1p4n$ channel of the present reaction. The proton tagging is therefore essential for the detection of the HD ridge. To clarify this point, statistical calculations have been performed modeling the decay of the compound nucleus ^{157}Ho from $J = 75\hbar$. We have verified that a difference exists between nuclei which decay emitting one proton and those emitting one neutron and survive fission in the first step of the deexcitation cascade. In fact the chance to survive fission in the second step is larger for the proton channel by a factor ~ 1.5 with respect to the channel having the neutron in the first step. This is due to the change in fissility and to the larger dissipation of excitation energy in the proton decay. We stress that the gain in survival probability is derived from standard "statical" statistical model calculations whose reliability at such high angular momentum is unknown. It is possible that the decay is substantially different from that predicted from the model since the protons are emitted from a transient system during its elongation toward the scission. Therefore, the emitter deformation should be substantially different from the equilibrium deformation used in statistical model calculations which can give large effects on the transmission coefficients and on the binding energies [25].

We note also that the increase of the proton energy for the HD states is not compatible with the argument used in the past to justify the importance of the proton tagging [1], which was based on the supposed larger sensitivity of the protons to the nuclear deformation because of the emission barrier. In fact, the reduction of the barrier should in principle give a higher yield of low-energy protons resulting in a net lowering of the average proton energy. This is not supported by the experimental proton spectra measured in the present experiment for SD, oblate, or prolate structures in ^{152}Dy.

An increase of the proton energy might also be obtained by increasing the K value in the level density parameter $a = A/K$, with respect to the values $K = 8$ MeV^{-1} normally used in the calculations. Such a change in the level density is in principle possible because of the change in deformation. However we note in the calculations that the increase of K favors the fission competition, lowering the survival probability at large angular momenta. It seems therefore that the change of the level density is scarcely compatible with the phenomena observed in the present experiment.

In conclusion, a self-consistent description of the 30 keV ridge observed in the 187 MeV ^{37}Cl on ^{130}Sn reaction seems to emerge from the present investigation supporting the hypothesis that relates the ridge to hyperdeformed shapes in ^{152}Dy. A new data set with improved statistic is necessary to search for discrete transitions as those proposed in [4] and to better define the associated entry state region. Particle energy spectra with good statistics are certainly needed in coincidence with SD and HD nuclear shapes for a better comprehension of the population mechanism of such exotic shapes.

ACKNOWLEDGMENTS

We thank the accelerator crew of the Tandem XTU in Legnaro for providing good beam quality and efficient operation during the experiment. Thanks are due also to A. Buscemi, M. Caldogno, R. Isocrate, and R. Zanon for skillful technical help in preparing the experiment. One of us (N.H.M.) would like to acknowledge financial support from CNPq-Conselho National de Desenvolvimento Cientifico e Tecnologico (Brazil).

[1] J. Dudek, T. Werner, and L. L. Riedinger, Phys. Lett. B **211**, 252 (1988).
[2] S. Aberg, Nucl. Phys. **A557**, 17c (1993).
[3] B. M. Nyako *et al.*, Phys. Rev. Lett. **52**, 507 (1984).
[4] A. Galindo-Uribarri *et al.*, Phys. Rev. Lett. **71**, 231 (1993).
[5] D. Bazzacco *et al.*, Phys. Lett. B **309**, 235 (1993), and references therein.

[6] G. Palameta and J. C. Waddington, Nucl. Instrum. Methods A **234**, 476 (1985).
[7] P. J. Twin *et al.*, Phys. Rev. Lett. **57**, 811 (1986).
[8] J. K. Johansson *et al.*, Phys. Rev. Lett. **63**, 2200 (1989).
[9] M. A. Bentley *et al.*, J. Phys. G **17**, 481 (1991).
[10] R. K. Choudhury *et al.*, Phys. Lett. **143B**, 74 (1984).
[11] F. Puehlhofer, Nucl. Phys. **A280**, 267 (1977).
[12] D. G. Sarantites *et al.*, Phys. Rev. Lett. **64**, 2129 (1990).
[13] D. J. Blumenthal *et al.*, Phys. Rev. Lett. **66**, 3121 (1991).
[14] T. L. Khoo *et al.*, Nucl. Phys. **A557**, 83 (1993).
[15] G. La Rana *et al.*, Phys. Rev. C **37**, 1920 (1988), and references therein.
[16] N. G. Nicolis and D. G. Sarantites, Phys. Rev. C **40**, 2422 (1989).
[17] A. Galindo-Uribarri, Prog. Part. Nucl. Phys. **28**, 463 (1992).
[18] N. N. Ajitanand *et al.*, Nucl. Instrum. Methods A **243**, 111 (1986), and references therein.
[19] K. Schiffer and B. Herskind, Nucl. Phys. **A520**, 521c (1990).
[20] P. J. Nolan, Nucl. Phys. **A553**, 107 (1993).
[21] D. J. Hinde *et al.*, Phys. Rev. C **45**, 1229 (1992).
[22] M. Thoennessen and G. Bertch, Phys. Rev. Lett. **71**, 4303 (1993).
[23] J. P. Lestone *et al.*, Nucl. Phys. **A559**, 277 (1993).
[24] A. Galindo-Uribarri, private communication.
[25] P. Froebrich and I. I. Gontchar, Nucl. Phys. **A556**, 281 (1993); and unpublished.